

# Caribbean Plants as Source of Novel Inhibitors for Main Protease, NSP-15, and RNA-dependent RNA polymerase (RdRp) of SARS-Cov-2

Arya Duncan, Juchara Margetson, Jada Roberts, Taquanna Baron, Neelam Buxani\*

Department of Chemical and Physical Sciences, College of Science and Mathematics, St. Thomas Campus, The University of the Virgin Islands, VI-00802, United States

## ABSTRACT

The Covid-19 pandemic with 74,299,042 confirmed cases including 1,669,982 deaths, reported worldwide by WHO (accessed 1:21 PM EST on 12/20/2020) is one of the most challenging situations the humankind is facing currently. Though some vaccines to treat this catastrophic disease have been developed on fast track, but still exploring the more potential alternative therapies is need of the hour. In search of new drug candidates to treat this pandemic, a structure based virtual screening study was carried out on the 125 compounds isolated from the native Caribbean medicinal plants like Aloe vera, Lemon grass, Moringa Olifera, and Lignum vitae, to determine their inhibitory potential against three main drug targets of SARS CoV-2; main protease (PDB ID: 6LZE), nsp 15 (PDB ID: 6WLC), and RNA-dependent RNA Polymerase (PDB ID: 7BV2) of SARS-CoV-2. The virtual screening workflow was performed using Schrodinger small molecule drug discover suite, in that compounds were prepared and docked in active sites of all three proteins. The co-crystallized ligand of every protein was used as a positive control and all docking scores were compared with it. Out of 125 compounds, 37 showed favorable docking interaction with the proteins compared to the native ligand. 13 compounds showed excellent docking score against 6LZE, out of that the most negative docking score (-11.962) was of rutin in compare to native ligand (-8.095), and it also showed more negative Prime MMGBSA binding energy-70.54 kcal/mol. In case of 7BV2, 35 compounds showed better docking results than the native ramdesivir (-4.566), docking score (-8.194) of vicienin-2 was best, it also exhibited almost same binding energy of complex (44.54 Kcal/mol) as ramdesivir. In case of 6 WLC, in site 1, orientin showed most negative dockings core (-10.896), while in site 2 swertiajaponin's docking score is-12.364. Pharmacokinetic (ADME) properties of 37 compounds were also calculated to ascertain the druglikeness of potential inhibitors. This study provides some lead molecules that might be helpful in designing drug for treating corona virus disease.

**Keywords:** Main protease; NSP-15: Nonstructural protein-15; RNA dependant RNA polymerase; Caribbean medicinal plants; Aloe vera; Lemon grass; Moringa Olifera; Lignum vitae

## INTRODUCTION

The novel coronavirus SARS CoV-2, better known as COVID-19, is a new strain that belongs to the SARS family. This family of viruses replicates by binding to ACE receptors of cells and entering them to replicate. The virus itself consists of 2 subunits, one which binds to the ACE receptor and the other than binds to the cell surface to anchor the virus. The virus is most commonly found in a mass population among animals however, the new strain, SARS CoV-2 has been able to thrive among humans. A study of the genomic structure of the different coronavirus strains found that the new strain shares 88% similarity with the bat strain of SARS

[1]. Reports state that the main mode of transmission for the SARS CoV-2 virus is through person-to-person contact specifically by way of droplets from an infected person coming into contact with a healthy host.

The trend of infection and symptom severity is directly linked to immune health whereby immunocompromised persons have a higher risk of infection and severe symptoms. Currently, 14 days is the known incubation period of the virus however there have been cases where the virus showed symptoms earlier or later than expected [2]. The main target of the virus is the respiratory system. As is common among the coronavirus family, symptoms presented

**Correspondence to:** Neelam Buxani, Department of Chemical and Physical Sciences, College of Science and Mathematics, St. Thomas Campus, The University of the Virgin Islands, VI-00802, United States; Tel: +1(340)-693-1682; E-mail: neelam.buxani@uvi.edu

**Received:** December 21, 2020; **Accepted:** January 04, 2021; **Published:** January 11, 2021

**Citation:** Duncan A, Margetson J, Roberts J, Baron T, Buxani N (2021) Caribbean Plants as Source of Novel Inhibitors for Main Protease, NSP-15, and RNA-dependent RNA polymerase (RdRp) of SARS-Cov-2. Drug Des. 10:173.

**Copyright:** © 2021 Duncan A, et al. This is an open-access article distributed under the terms of the Creative Commons Attribution License, which permits unrestricted use, distribution, and reproduction in any medium, provided the original author and source are credited.

include a dry coughing, fever, and fatigue however this new strain presented symptoms particular to the virus [3]. In addition to the aforementioned, SARS CoV-2 also caused disruption as the lower airway such as sneezing and sore throat in addition to gastrointestinal symptoms which are rare for the coronavirus family [3].

Due to how infectious the virus is, social distancing and mask regulations have been implemented leading to the shutdown or heavy patron restriction of closed spaces. Because of this disruption in day to day life, treatment for or immunity to the virus is necessary. Common methods of drug development take an extensive amount of time which is what makes computer-aided drug design a favorable computational tool. Computer-aided drug design is a computation drug design method that involves identifying active sites of target proteins and simulating protein-compound interactions to find inhibitors. The two types of computational drug design are structure-based drug design and ligand-based drug design [4]. Ligand-based drug design is used when the ligand structure is known but the receptor structure is unknown. Structure-based drug design on the other hand involves analyzing the known receptor structure to identify potential active sites, if unknown, and simulate ligand interactions at those sites to identify potential inhibitors that can compete with the biological ligand [4].

There are different proteins that are associated with SARS CoV-2 functionality that are potential drug targets. Inhibition of these proteins could render the virus ineffective as interactions and mechanisms would be disrupted. The main protease (Mpro) is an essential drug target which, along with papain-like proteases catalyzes the processing of polyproteins translated from viral RNA and recognizes specific cleavage sites [5]. The RNA dependent RNA polymerase (RdRp) has been evident to possess nsp (7,8,12); each RdRp acts as responsive cofactors when stimulating polymerase complex activities. The CoV nsp7/nsp8/nsp12 complex constitutes nucleotide polymerization for its configuration [6]. In addition, the nsp 15 (active hexamer) is responsible for providing structural attributes for the development of innovative therapeutic agents [7]. The SARS-CoV-2 polyprotein assists with transportation mechanisms functioning with maintenance, transcription, and replication of the virus genome.

In this study, four medicinal plants aloe vera, lemon grass, Moringa oleifera and Lignum vitae native to the Caribbean were chosen to determine the inhibitory effects of the antiviral compounds isolated from them on different SARS CoV-2 proteins. Based on the literature [8-11] a list of 125 compounds were compiled in Table 1 and were virtually docked in the active sites of Main protease, RNA dependent RNA Polymerase, and nsp-15 proteins of SARS-CoV-2 by using molecular docking program (GLIDE, Schrodinger). Docking scores and binding energies of protein-ligand complexes were compared with the native ligand of the chosen protein structures. ADME properties of selected compounds were also determined.

**Table 1:** Complete list of compounds and their origin.

S. No.	Compounds	Plant Origin
1	Chrysophanol	Aloe Vera
2	C-2'-decoumaroyl-aloesin G	Aloe Vera
3	Aloe emodin	Aloe Vera

4	Aloe C-glucosylchromone	Aloe Vera
5	Aloin	Aloe Vera
6	4-methylpent-3-en-1-ol	Aloe Vera
7	4,7-dihydroxy-5-methylcoumarin	Aloe Vera
8	Aloe emodin anthrone	Aloe Vera
9	Ruxolitinib phosphate	Aloe Vera
10	Ruxolitinib	Aloe Vera
11	Aloesin	Aloe Vera
12	6-Methyl-1,3,8-trihydroxyanthraquinone (emodin)	Aloe Vera
13	Luteolin-8-C-glucoside (orientin)	Aloe Vera
14	Feruloylquinic acid	Aloe Vera
15	10-Hydroxyaloin A	Aloe Vera
16	Isovitexin	Aloe Vera
17	Isoaloesin D	Aloe Vera
18	Aloin B	Aloe Vera
19	5,3'-Dihydroxy-6,7,4'-trimethoxyflavone (eupatorin)	Aloe Vera
20	Trihydroxy octadecenoic acid	Aloe Vera
21	3,4-Di-O-caffeoylquinic acid	Aloe Vera
22	6-methylhept-5-en-2-one	Lemon Grass
23	Camphene	Lemon Grass
24	Limonene	Lemon Grass
25	Nonan-4-ol	Lemon Grass
26	Citronellal	Lemon Grass
27	Citronellol	Lemon Grass
28	Neral	Lemon Grass
29	Geraniol	Lemon Grass
30	Citral	Lemon Grass
31	Geranyl acetate	Lemon Grass
32	$\beta$ -caryophyllene	Lemon Grass
33	$\gamma$ -muurolene	Lemon Grass
34	Caryophyllene oxide	Lemon Grass
35	Swertiajaponin	Lemon Grass
36	7-epi-ent-eudesmane-5,11-diol	Lemon Grass
37	(2E,6E)-hedycaryol	Lemon Grass
38	1,2-Benzenedicarboxylic acid, mono(2-ethylhexyl) ester	Moringa Oleifera
39	1,3-dibenzyl urea	Moringa Oleifera
40	2-Ethyl-2-propyl-1-hexanol	Moringa Oleifera
41	3,3-dimethyloctane	Moringa Oleifera
42	4- Dodecanol	Moringa Oleifera
43	4-(L-rhamnopyranosyloxy) benzyl glucosinolate (glucomoringin)	Moringa Oleifera
44	4,6,8-Trimethyl-1-nonene	Moringa Oleifera
45	All-E-lutein	Moringa Oleifera
46	All-E-Zeaxanthin	Moringa Oleifera
47	-Phellandrene	Moringa Oleifera
48	Apigenin	Moringa Oleifera
49	Arachidic acid	Moringa Oleifera
50	Astragaln	Moringa Oleifera

51	Aurantiamide acetate	Moringa Oleifera
52	Behenic acid	Moringa Oleifera
53	Benzyl glucosinolate (glucotropaeolin)	Moringa Oleifera
54	Benzylamine	Moringa Oleifera
55	$\beta$ -sitosterol	Moringa Oleifera
56	Caffeic acid	Moringa Oleifera
57	Chlorogenic acid	Moringa Oleifera
58	Cryptochlorogenic acid	Moringa Oleifera
59	D-allose	Moringa Oleifera
60	Dibutyl phthalate	Moringa Oleifera
61	Ellagic acid	Moringa Oleifera
62	Epicatechin	Moringa Oleifera
63	Eugenol	Moringa Oleifera
64	Ferulic acid	Moringa Oleifera
65	Gallic acid	Moringa Oleifera
66	Genistein	Moringa Oleifera
67	Gentisic acid	Moringa Oleifera
68	Glucosylrutin	Moringa Oleifera
69	Glucosylrutin(1-)	Moringa Oleifera
70	Henriactone	Moringa Oleifera
71	Hexanedioic acid, bis (2-ethylhexyl)	Moringa Oleifera
72	Isoquercetin	Moringa Oleifera
73	Isorhamnetin	Moringa Oleifera
74	Kaempferol	Moringa Oleifera
75	Kaempferol-3-O-rhamnoside	Moringa Oleifera
76	Kaempferol-3-O-glucoside	Moringa Oleifera
77	Kaempferol-3-rutinoside	Moringa Oleifera
78	Linoleic acid	Moringa Oleifera
79	Linolenic acid	Moringa Oleifera
80	Luteolin	Moringa Oleifera
81	Marumosi A	Moringa Oleifera
82	Marumosi B	Moringa Oleifera
83	Moringyne	Moringa Oleifera
84	Multiflorin B	Moringa Oleifera
85	Myricetin	Moringa Oleifera
86	Myristic acid	Moringa Oleifera
87	N-L-rhamnopyranosyl vicosamide	Moringa Oleifera
88	Niazimicin	Moringa Oleifera
89	Niaziminin	Moringa Oleifera
90	Niazirin	Moringa Oleifera
91	Niazirin	Moringa Oleifera
92	o-Coumaric acid	Moringa Oleifera
93	O-ethyl-4-[(L-rhamnosyloxy)-benzyl] carbamate	Moringa Oleifera
94	Oleic acid	Moringa Oleifera
95	p-Coumaric acid	Moringa Oleifera
96	p-Cymene	Moringa Oleifera
97	Palmitoleic acid	Moringa Oleifera
98	Procyanidin	Moringa Oleifera
99	Pterygospemin	Moringa Oleifera
100	Quercetin	Moringa Oleifera

101	Rutin	Moringa Oleifera
102	Salicylic acid	Moringa Oleifera
103	Sinabin	Moringa Oleifera
104	Sinapic acid	Moringa Oleifera
105	Squalene	Moringa Oleifera
106	Stearic acid	Moringa Oleifera
107	Syringic acid	Moringa Oleifera
108	Tetracontane-1,40-diol	Moringa Oleifera
109	Trimethyl (4-tert-butylphenoxy)silane	Moringa Oleifera
110	Vanillin	Moringa Oleifera
111	Vicenin-2	Moringa Oleifera
112	Z,Z-2,5-Pentadecadien-1-ol	Moringa Oleifera
113	Ramonanin A	Lignum Vitae
114	Ramonanin B	Lignum Vitae
115	Ramonanin C	Lignum Vitae
116	Ramonanin D	Lignum Vitae
117	Gingerone B	Lignum Vitae
118	Glucoputranjivin(1-)	Lignum Vitae
119	$\beta$ -sesquiphellandrene	Lignum Vitae
120	Glucoputranjivin	Lignum Vitae
121	Pinocarveol	Lignum Vitae
122	(2E,6E)-hedycaryol	Lignum Vitae
123	Dodecane	Lignum Vitae
124	Zingiberene	Lignum Vitae
125	all-cis-octadeca-6,9,12,15-tetraenoic acid	Lignum Vitae

## MATERIALS AND METHODS

The virtual screening and molecular docking were performed using the Schrodinger small molecule drug discovery suite, Schrödinger Release 2020-2: Schrödinger, LLC, New York, NY, 2020.

### Protein preparation and receptor grid generation

The COVID-19 proteins, main protease (PDB ID: 6LZE), RNA dependent RNA polymerase (PDB ID: 7BV2) and nsp-15 (PDB ID: 6WLC) were retrieved from the Protein Data Bank [12,13]. Using Schrodinger's Protein Preparation Wizard the imported proteins were preprocessed, optimized, and minimized. During preprocessing of proteins missing hydrogens and residues were added with the help of Prime (version). As there was a bound ligand with all these proteins, so the receptor grids with the dimensions 10 Å × 10 Å × 10 Å were generated by selecting the atom of ligand molecule using Schrodinger receptor grid version 8.7.

### Ligand preparation

A total of 4 medicinal plants native to the Caribbean were selected to compile a list of compounds to be virtually screened and identify potential antiviral agents for COVID-19. A literary analysis of numerous research papers and screening of databases generated compounds from each of the 4 plants for a total of 125 compounds (Table 1). The 2D chemical structures of all compounds discovered were imported from the PubChem database in SDF format into Maestro. Using Schrodinger's LigPrep module, all the compounds were converted into 3D structures and optimized under Force field OPLS3e, different ionization states were generated at pH 7.0±2.0 using Epik module (version 5.2) Specific chiralities of

3D structures were retained, while around other chiral centers all possible stereoisomers were generated. Total 153 structures were taken to the docking analysis.

In present study, co-crystallized ligand of each protein was used as reference ligand; a peptide inhibitor {N}[(2~{S})-3-cyclohexyl-1-oxidanylidene-1-[(2~{S})-1-oxidanylidene-3-(3~{S})-2-oxidanylidene-pyrrolidin-3-yl]propan-2-yl]amino]propan-2-yl]-1~{H}-indole-2-carboxamide (FHR) (Figure 1a) of main protease, Ramdesivir (Figure 1b) as an inhibitor of RdRp, and Uridine-5'-monophosphate (Figure 1c) inhibitor of nsp-15.

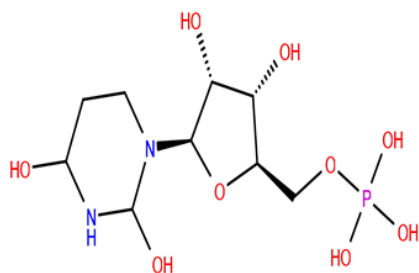


**Figure 1a:** {N}[(2~{S})-3-cyclohexyl-1-oxidanylidene-1-[(2~{S})-1-oxidanylidene-3-(3~{S})-2-oxidanylidene-pyrrolidin-3-yl]propan-2-yl]amino]propan-2-yl]-1~{H}-indole-2-carboxamide (FHR).

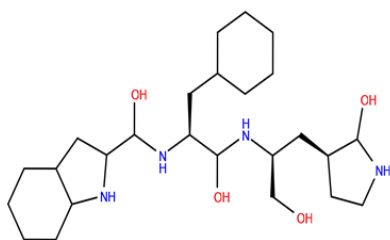


**Figure 1b:** Ramdesivir.

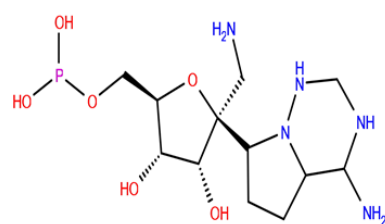


**Figure 1c:** Uridine-5'-monophosphate.

## Molecular docking

Using Glide Standard Precision (SP) the interaction between each protein and the 153 compounds and native ligand were analyzed. Based on the binding affinity scores generated (docking score), the compounds that had scores close to or better than the native ligand were selected for Extra Precision (XP) docking. Of the 153 docked compounds those with docking scores better than the native ligand for the protein were selected for further screening in XP mode along with the native ligand. If no compounds had a better docking score than the native ligand, compounds with glide

scores-6.00 were chosen and further screened. The docking scores were again analyzed to determine which compounds, if any, have a higher affinity than the native ligand.

Further analysis of the compounds was necessary to determine the binding energy of protein-ligand complexes. With the knowledge of which compounds and poses best interacted with the protein, the compounds from XP mode were analyzed using Prime MM-GBSA. The SP and XP docking results showed that the various compounds interact with the protein and bind to the active site while Prime-MM-GBSA shows the free binding energy of the ligand-protein association.

## ADME properties

The conclusion of the molecular docking study identified different compounds that interact well with the protein in comparison to the respective native ligand. Using QikProp (v6.4) of the Maestro (v12.4), the ADME properties of the top docking scorers were analyzed to determine if any of the compounds showed drug-like properties.

## RESULTS AND DISCUSSION

### Structure-based virtual screening

Using the binding site of the native ligand, FHR, bound to the main protease 6LZE, a receptor grid of the active site was generated to dock the researched 125 compounds. An analysis of the active site showed the native ligand interaction *via* hydrogen bonds (H-Bond) with the GLY 143, PHE 140, HIE 163, and GLU 166 residues (Figures 2a-2c). Ligand preparation of the 125 researched compounds generated a total of 153 different poses to be filtered with all 153 meetings the filter parameters. Because of the small compound library, preliminary virtual screening was carried out in SP mode and a total of 38 compounds were filtered out based on their docking score. The SP mode docking results did not yield any compounds with a docking score better than the native (docking score=-9.734) so all compounds with scores equal to or greater than-6.00 were selected for XP virtual screening.

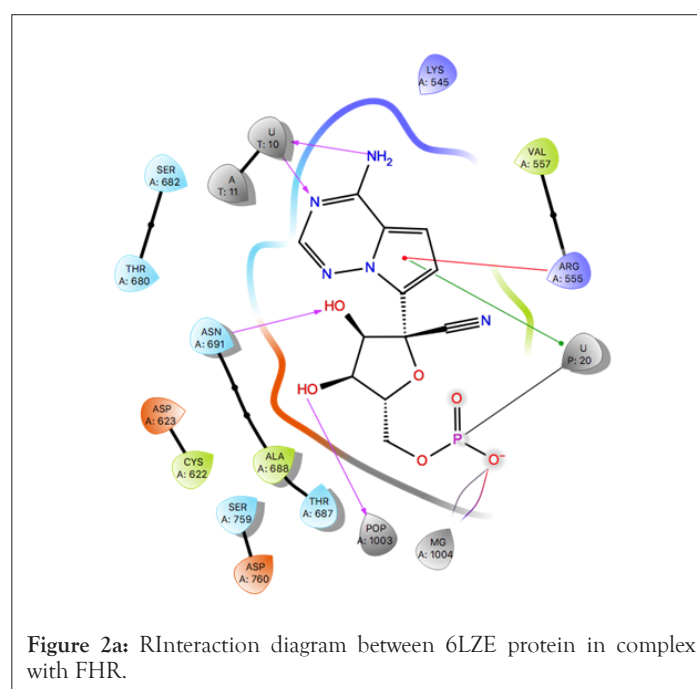


**Figure 2a:** RInteraction diagram between 6LZE protein in complex with FHR.

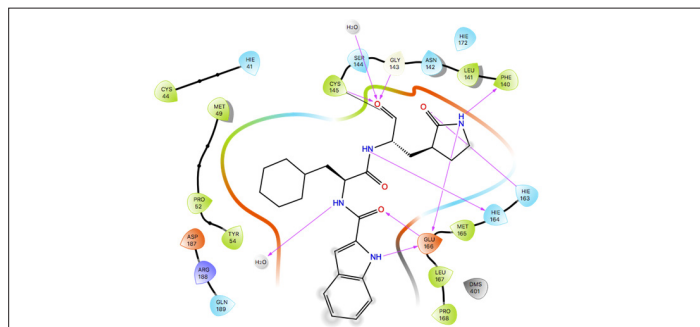


**Figure 2b:** Interaction diagram between 7BV2 protein in complex with Remdesivir.

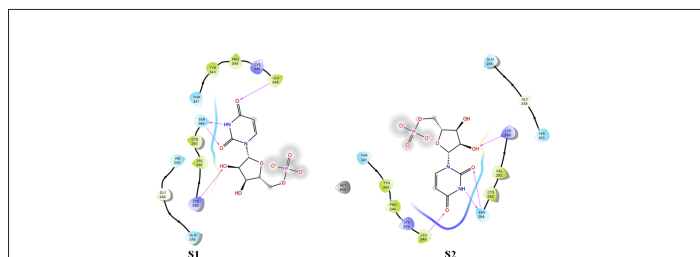


**Figure 2c:** Interaction diagram between 6WLC protein in complex with Uridine-5'-Monophosphate (site 1 and 2 left to right).

Like the 6LZE protein, 7BV2 and 6WLC had their active site analyzed and the compounds docked to those sites in SP mode to determine top scorers. There were 40 compounds that had better docking scores than the native ligand when docked in SP mode to 7BV2. On the other hand, because 6WLC had 2 different sites, the compounds were docked in SP mode to both. Site 1 did not produce any compounds that had better docking scores than the native so all compounds with SP scores  $>6.00$  were selected for XP docking. Site 2 on the other hand had 18 compounds with better docking scores than the native in SP mode. All compounds that scored better than the native or had an SP docking score  $>6.00$  when no better interactions were produced were docked to their respective sites in XP mode.

The XP docking method was able to provide positive results as it showed there were compounds that interacted better than the native ligand. The XP docking yielded multiple compounds that had a better docking score than the native ligand for each protein (Tables 2-4).

**Table 2:** Top scoring compounds from 6LZE docking.

Compounds	XP docking score	Molecular Weight	Prime MMGBSA dG Bind (kcal/mol)
Rutin	-11.962	610.524	-70.54
Vicenin-2	-10.001	594.525	-60.39
Procyanidins	-9.747	594.528	-56.41
Kaempferol-3-Rutinoidide	-9.388	594.525	-47.29
Astragalin	-9.369	448.382	-42.34
Kaempferol-3-O-Glucoside	-9.369	448.382	-42.34
10-Hydroxyaloin A	-9.217	434.399	-54.61
Marumosiide B	-9.031	459.449	-23.83
Multiflorin B	-9.045	594.525	-22.96

Orientin	-8.554	448.382	-54.66
Chlorogenic Acid	-8.373	354.313	-18.06
Kaempferol-3-O-Rhamnoside	-8.354	756.667	-40.47
Aloin	-8.233	418.399	-52.31
FHR	-8.095		-69.71

**Table 3:** Top Scoring Compounds from 7BV2 docking.

Compounds	XP docking score	Molecular Weight	Prime MMGBSA dG Bind (kcal/mol)
Vicenin-2	-8.194	594.525	-44.54
Multiflorin B	-7.657	594.525	-29.57
Marumosiide B	-7.591	459.449	-38.5
3,4-Di-O-Caffeoylquinic Acid	-7.585	516.457	-39.88
N-Alpha-L-Rhamnopyranosyl Vicosamide	-7.468	660.674	-39.3
Isoquercetin	-7.467	464.382	-32.69
Swertiajaponin	-7.245	462.409	-29.12
Orientin	-7.09	448.382	-48.84
Kaempferol-3-Rutinoidide	-7.008	594.525	-41.88
Aloin	-6.912	418.399	-41.95
Glucotropeolin	-6.561	409.425	-22.07
Chlorogenic Acid	-6.412	354.313	-22.96
Astragalin	-6.337	448.382	-32.72
Kaempferol-3-O-Glucoside	-6.337	448.382	-32.72
D-Allose	-6.184	180.157	-15.92
Sinalbin	-6.18	425.425	-28.97
Niazimicin	-6.147	357.421	-19.05
Isoaloeresin D	-6.136	556.565	-42.16
Cryptochlorogenic Acid	-6.017	354.313	-27.31
Glucoconringiin	-6.004	391.408	-20.93
Glucoconringiin 1_	-6.004	391.408	-20.93
Glucoputranjivin	-5.971	361.381	-22.8
Glucoputranjivin 1	-5.971	361.381	-22.79
Isovitexin	-5.987	432.383	-30.58
10-Hydroxyaloin A	-5.925	434.399	-30.2
Isorhamnetin	-5.645	316.267	-9.1
Aloesin	-5.617	394.377	-34.93
Kaempferol-3-O-Alpha-Rhamnoside	-5.406	756.667	-37.95
Moringyne	-5.286	312.319	-20.33
Niaziminin	-4.984	399.458	-35.99
Niazirin	-4.915	279.292	-32.1
Caffeic Acid	-4.848	180.16	-22.94
Aloe Emodin Anthrone	-4.815	256.257	-16.68
Gallic Acid	-4.798	170.121	-18.32
O-Ethyl-4-[(Alpha-L-Rhamnopyranosyloxy)-Benzyl] Carbamate	-4.635	357.36	-29.36
Remdesivir (Native)	-4.566		-44.66

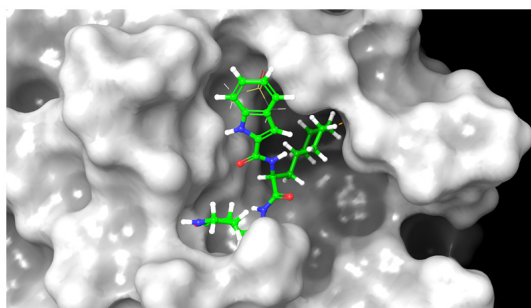
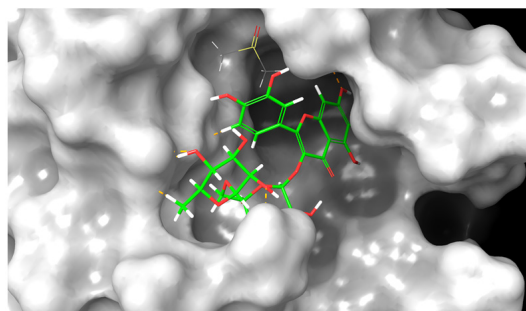
**Table 4:** Top scoring compounds from 6WLC docking.

	XP docking score	Molecular Weight	Prime MMGBSA dG Bind (kcal/mol)
Orientin S1	-10.896	448.382	-10.24
Uridine-5'-Monophosphate S1	-9.035		0
Swertiajaponin S2	-12.364	462.409	-10.24
Glucoconringiin S2	-11.691	391.408	0
Sinalbin S2	-11.543	425.425	0
Glucoconringiin 1- S2	-11.153	391.408	0
Aloesin S2	-10.411	394.377	-10.24
Uridine-5'-Monophosphate S2	-10.325		0
6WLC has 2 binding sites. The corresponding site for the compound is denoted as S1 (site 1) and S2 (site 2)	-4.566	-4.566	-4.566

**Table 5:** H-bonding interactions of Top Scoring Compounds with different residues of 6WLC.

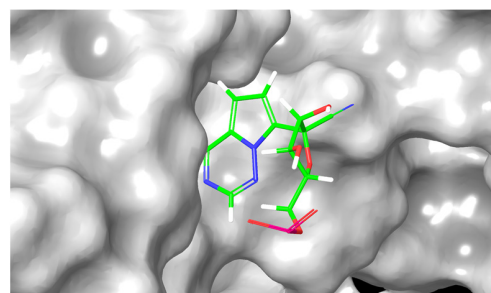
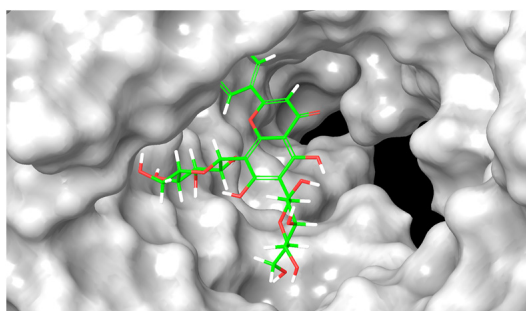
Compounds	Residues forming H-Bonding
Orientin	SER 294, GLN 245, THR 341, HIS 250, HIS 235
Swertiajaponin	SER 294, LYS 290, LYS 174, GLU 146, LEU 346, ASP 17
Glucoconringiin	TYR 343, SER 294
Sinbalin	SER 294, VAL 292
Glucoconringiin 1	GLU 146, LYS 174, SER 294, LYS 65
Aloesin	HIS 235, GLN 245, GLU 146, LYS 65

The 6LZE protein had 13 compounds that docked better than the native ligand. These 13 interactions were analyzed using Prime MM-GBSA to determine the binding energy. Glide XP and Prime MM-GBSA scores for the top 13 compounds can be found in Table 2. The most prominent interaction between the protein-ligand complex was hydrogen bonding. In almost all complexes, hydrogen bonding occurred between the compound and the GLU 166 residue as is present in the native ligand-protein complex. This is the only common interaction when comparing the native ligand and the tested compounds, however when comparing the test compounds, hydrogen bonding with the CYS 145 residue and pi-pi stacking interaction between the HIE 41 residue and benzene derivatives are prominent (Figures 3a and 3b).

**Figure 3a:** 6LZE with FHR native ligand.**Figure 3b:** 6LZE with Rutin (top XP scorer).

The Prime MM-GBSA analysis showed the free binding energy of each compound-protein complex. The top 13 compounds had a range of free binding energy from -18.06 kcal/mol to -70.54 kcal/mol. The complex with the lowest energy, which is most favorable, belongs to Rutin which also has better binding energy than the native ligand which would suggest a potentially strong inhibitor of the main protease. Rutin also had the best docking score at -11.962. The ligand interaction diagram shows H-Bonds with GLY 143 and GLU 166 residues the same as the native ligand but also interacts *via* hydrogen bonding with ASN 142, CYS 145, HIE 41, and GLN 189.

A total of 36 compounds had better ligand interactions than the native ligand of 7BV2. Similar to 6LZE, the main interactions between the protein and the ligands is hydrogen bonding. The native ligand interacts with the protein by hydrogen bonds with ASN 691, U10, POP 1003 and ring interactions with U 20 and ARG 555. The binding energy for the top compounds range from -9.1 to -48.84. The compound Orientin has the most favorable Prime-MM GBSA binding energy (-48.84) and has a better docking score than the 7BV2 native ligand. The ligand interaction diagram for Orientin shows that its interaction with the protein is strictly *via* hydrogen bonding with A 11, U 12, A 13, A 12, A 14, C 15, ASN 496 (Figures 4a and 4b).

**Figure 4a:** 7BV2 with Remdesivir native ligand.**Figure 4b:** 7BV2 with Vicenin-2 (top XP scorer).

An analysis of the docking results for the 6WLC protein shows that one site has more favorable interactions with the compounds than the others. Only 1 of the 125 compounds interacts more favorably at site 1 (S1) than the native. Site 2 (S2) on the other hand had favorable interactions with 5 compounds (Table 4). The native ligand, Uridine-5'-Monophosphate, interacted with the protein *via* hydrogen bonding with LYS 65, ILE 64, SER 294 and LEU 346. Comparison of the native ligand interaction and the tested compounds shows that there are many residues in common between them. The tested compounds all form hydrogen bonds with at least one of the same residues as the native suggesting their importance in the active site and compound interactions (Figures 5a and 5b).

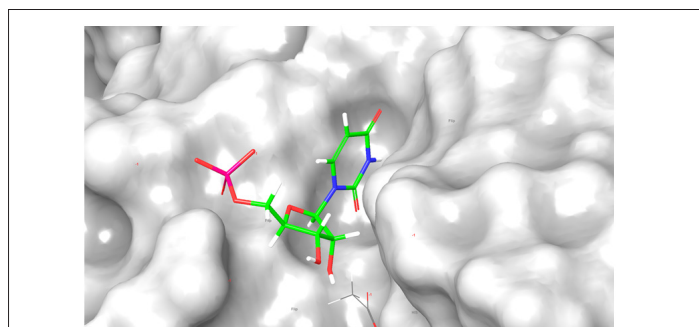


Figure 5a: 6WLC with Uridine-5'-Monophosphate native ligand.

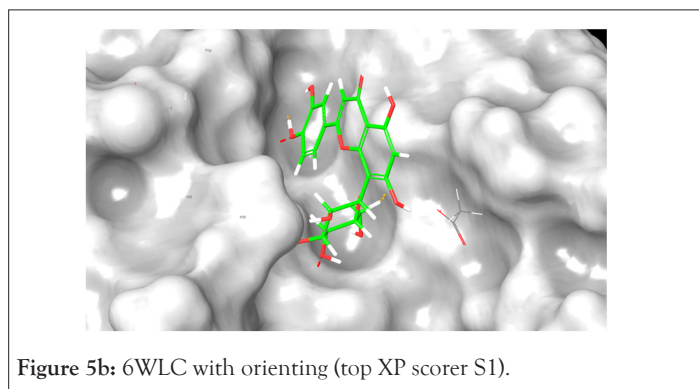


Figure 5b: 6WLC with orientin (top XP scorer S1).

In addition to the docking score, Prime MMGBSA analysis shows that these compounds have the most favorable binding energy out of all the protein-ligand interactions. The binding energy for the native ligand is 0 kcal/mol for both sites. Of the 6 total ligands

that interacted with the protein irrespective of site, half have equal binding energy to the native and the other half have better binding energy than the native at -12.04 kcal/mol. The common residue interaction among all compounds aside from Aloesin is the SER 294 residue, suggesting it is a key residue in ligand interaction in the active site. A complete list of H-bonding interactions for the top scoring compounds is given in Tables 2- 5.

Among all the compounds, one showed promising interaction with all three proteins. Orientin, a compound native to Aloe Vera, not only showed docking scores that were better than the native ligand for all proteins but also had a better binding affinity to the protein than the native. It showed higher affinity with the 7BV2 and 6WLC proteins and had a similar score for 6LZE. Prime MMGBSA and XP docking scores for Orientin and each protein's native ligands can be found in their respective Tables 2-4 for 6LZE, 7BV2 and 6WLC respectively Table 6.

### ADME properties

The 13 best compounds from molecular docking went through ADME analysis using the QikProp module on Maestro. A total of 11 properties were the main focus which include the molecular weight, the number of hydrogen donors, the number of hydrogen acceptors, the number of violations of the rule of five, predicted IC50 value for blockage of HERG K<sup>+</sup> channels (QPlogHERG), percent human oral absorption, predicted aqueous solubility (QPlogS), prediction of binding to human serum albumin (QPlogKhsa), predicted octanol/water partition coefficient (QPlogPo/w), predicted blood/brain partition coefficient (QPlogBB), number of likely metabolic reactions (#metab), and predicted apparent Caco-2 cell permeability (QPpCaco-).

ADME analysis showed that each compound has its pros and cons with no one compound falling within the acceptable range for all the properties. Most of the compounds had at least 1 violation of the rule of five with a few that had no violations. Lipinski Rule of Five states that drug-like compounds should have molecular weight lower than 500, lipophilicity (logP) lower than 5, less than five hydrogen bond donors, and less than 10 hydrogen bond acceptors, but many of natural products drugs do not comply with the "Rule of Five" [14]. It is recommended to not apply overly rigid cut-off points, as it increases the risk of losing some valuable compounds in earlier stages of screening [14], especially in case of natural products. A comprehensive list of the compounds and their ADME properties can be found in Table 6.

Table 6: ADME Properties.

Compound	Rule of 5	Donor HB	Accept HB	% Human oral absorption	QPlogS	QPlogPo/w	QPlogKhsa	#metab	QPlogHERG	QPpCaco	QPlogBB
Rutin	3	9	20.55	0	-2.114	-2.536	-1.293	10	-5.217	1.158	-4.419
Vicenin-2	3	10	20.75	0	-3.016	-2.851	-1.333	15	-6.03	0.498	-5.182
Procyanidins	3	10	11.65	0	-3.622	0.082	-0.394	12	-5.892	1.024	-4.313
Kaempferol-3-rutinoside	3	8	19.8	0	-3.129	-1.944	-1.281	9	-6.392	1.458	-4.813
Astragaln	2	6	13	11.182	-2.741	-0.822	-0.79	7	-5.422	6.86	-3.27
Kaempferol-3-O-glucoside	2	6	13	11.182	-2.741	-0.822	-0.79	7	-5.422	6.86	-3.27
10-Hydroxyaloin A	1	6	12.45	22.877	-2.58	-0.895	-0.753	11	-4.86	6.16	-3.219
Marumoside B	2	8	18.55	0	-0.849	-3.009	-1.674	8	-3.63	4.509	-3.442
Multiflorin B	3	8	19.8	0	-2.513	-2.031	-1.225	9	-5.74	1.681	-4.334
Orientin	2	7	13	5.071	-2.752	-1.178	-0.747	10	-5.024	4.084	-3.343

Chlorogenic acid	1	6	9.65	17.723	-2.532	-0.239	-0.932	5	-3.304	1.936	-3.291
Kaempferol-3-O-rhamnoside	3	11	28.3	0	-2.411	-4.255	-2.13	12	-6.635	0.09	-7.139
Aloin	1	5	11.7	30.587	-2.657	-0.392	-0.623	11	-4.693	11.367	-2.803
3,4-Di-O-caffeoylquinic acid	3	7	11.45	1	-4.307	0.812	-0.628	6	-4.935	0.199	-5.305
N-alpha-L-rhamnopyranosyl vincosamide	3	7	23.9	1	-2.218	-1.998	-1.346	11	-6.917	1.673	-3.594
isoquercetin	2	7	13.75	1	-2.68	-1.394	-0.874	8	-5.379	2.192	-3.894
swertiajaponin	2	6	13	1	-3.292	-0.531	-0.696	10	-5.544	9.208	-3.205
Glucotropeolin	0	5	14	1	-1.37	-1.098	-1.339	6	-2.64	2.314	-3.061
D-allose	0	5	10.2	2	-1.045	-2.211	-0.873	4	-2.7	67.286	-1.569
Sinalbin	2	6	14.75	1	-1.404	-1.559	-1.396	7	-2.608	0.954	-3.515
niazimicin	0	4	9.55	3	-3.631	1.179	-0.483	4	-5.179	264.212	-1.521
Isoaloesin D	2	5	14.5	1	-3.783	1.588	-0.342	10	-5.402	59.493	-2.531
Cryptochlorogenic acid	1	6	9.65	2	-2.115	-0.179	-0.913	5	-2.774	3.012	-2.857
glucoconringiin	2	6	14.75	1	-1.458	-1.837	-1.511	7	-2.598	1.314	-3.661
glucoconringiin 1-	2	6	14.75	1	-1.458	-1.837	-1.511	7	-2.598	1.314	-3.661
Glucoputranjivin	0	5	14	2	-1.392	-1.477	-1.412	6	-2.241	3.359	-2.961
Glucoputranjivin 1	0	5	14	2	-1.392	-1.477	-1.412	6	-2.241	3.359	-2.961
Isovitexin	1	6	12.25	2	-3.29	-0.591	-0.671	9	-5.688	8.105	-3.185
isorhamnetin	0	3	5.25	3	-3.458	1.232	-0.152	5	-5.169	59.672	-1.952
Aloesin	0	5	13.75	2	-2.747	-1.03	-0.884	9	-4.726	22.527	-2.648
Moringyne	0	4	10.5	3	-2.22	-0.087	-0.767	6	-4.43	212.456	-1.449
niaziminin	0	3	9.85	3	-5.202	2.314	-0.207	3	-5.984	387.686	-1.461
Niazirin	0	3	9.05	3	-3.062	-0.003	-0.75	4	-4.469	145.234	-1.608
Caffeic acid	0	3	3.5	2	-1.369	0.562	-0.792	2	-2.197	21.699	-1.576
Aloe emodin anthrone	0	1	3.2	3	-3.205	2.016	0.027	4	-4.568	224.785	-1.188
Gallic acid	0	4	4.25	2	-0.701	-0.567	-0.983	3	-1.417	10.04	-1.662
O-ethyl-4-(alpha-L-rhamnosyloxy)-benzyl carbamate	0	5	8.6	3	-3.142	0.681	-0.468	4	-4.952	65.672	-2.232

## CONCLUSION

The researched plants are all used for medicinal purposes in the Caribbean from centuries. Based on the present in-silico study, multiple compounds showed promising inhibitory potential against different SARS CoV-2 proteins. Some of the compounds like rutin, vicenin-2, and Orientin exhibited better protein-compound association in compare to respective native ligands and found to have more negative binding energy. Further research on the antiviral properties of these plants against the various proteins of the SARS CoV-2 virus could prove useful for the discovery of naturally occurring antiviral compounds for future drugs and may provide natural remedies against this fatal disease.

## REFERENCES

- Chen Y, Guo Y, Pan Y, Zhao ZJ. Structure Analysis of the Receptor Binding of 2019-NCoV. *Biochem Biophys Res Commun.* 2020; 525(1):135-140.
- Sauer LM. What Is Coronavirus? *Johns Hopkins Med J.* 2020.
- Rothan HA, Byrareddy SN. The Epidemiology and Pathogenesis of Coronavirus Disease (COVID-19) Outbreak. *J Autoimmun.* 2020; 109:102433.
- Yu W, Mackerell AD. Computer-Aided Drug Design Methods. *Methods in Molecular Biology Antibiotics.* 2016; 85-106.
- Gurung AB, Ali MA, Lee JK, Farah MA, Al-Anazi KM. Unravelling lead antiviral phytochemicals for the inhibition of SARS-CoV-2 Mpro enzyme through in silico approach. *Life Sci.* 2020; 255:117831.
- Kirchdoerfer RN, Ward AB. Structure of the SARS-CoV nsp12 polymerase bound to nsp7 and nsp8 co-factors. *Nat Commun.* 2019; 10(1):1-9.
- Pillon MC, Frazier MN, Dillard L, Williams JG, Kocaman S, Krahn JM, et al. Cryo-EM Structures of the SARS-CoV-2 Endoribonuclease Nsp15. *BioRxiv.* 2020.
- Quispe C, Villalobos M, Bórquez J, Simirgiotis M. Chemical Composition and Antioxidant Activity of Aloe Vera from the Pica Oasis (Tarapacá, Chile) by UHPLC-Q/Orbitrap/MS/MS. *J Chem.* 2018; 2018:1-12.
- Abd Rani NZ, Husain K, Kumolosasi E. Moringa genus: A review of phytochemistry and pharmacology. *Front Pharmacol.* 2018; 9:108.
- Nasr-Eldin MA, Abdelhamid A, Baraka D. Antibiofilm and antiviral potential of leaf extracts from *Moringa oleifera* and rosemary (*Rosmarinus officinalis lam.*). *Egypt J Microbiol.* 2017; 52(1):129-139.

11. Team EBIW. Chemical Entities of Biological Interest (ChEBI). 2020.
12. Zhang B, Zhang Y, Jing Z, Liu X, Yang H, Liu H, et al. 6LZE: The crystal structure of COVID-19 main protease in complex with an inhibitor 11a. PDB. 2020.
13. Kim Y, Maltseva N, Jedrzejczak R, Endres M, Chang C, Godzik A et al. 6WLC: Crystal Structure of NSP15 Endoribonuclease from SARS CoV-2 in the Complex with Uridine-5'-Monophosphate. RCSB PDB. 2020.
14. Lionta E, Spyrou G, K Vassilatis D, Cournia Z. Structure-based virtual screening for drug discovery: principles, applications and recent advances. *Curr Top Med Chem.* 2014; 14(16):1923-1938.